Tokyo Climate Center, Japan Meteorological Agency

TCC News

Spring 2021

Table of Contents: TCC News No. 64

El Niño Outlook (June - December 2021)

The La Niña event that started in summer 2020 has terminated. ENSO-neutral conditions are likely to continue through to next autumn (60%).

1. El Niño/La Niña

In May 2021, the NINO.3 SST was below normal with a deviation of -0.5°C. The five-month running mean of the NINO.3 SST deviation was -0.6°C in March 2021, constituting 9 consecutive months of -0.5°C or below SST beginning last July (this satisfies JMA's criterion of a La Niña event of -0.5°C or below for consecutive 6 months). SSTs in the equatorial eastern Pacific, though still below normal, were gradually nearing to normal throughout the month (Figure 1-1). Subsurface temperatures were above normal in the western and central parts and near normal in the eastern parts (Figure 1-2 and 1-3). While easterly winds in the lower troposphere (i.e., trade winds) over the central equatorial Pacific were stronger than normal, atmospheric convective activity near the date line over the equatorial Pacific was near normal. As these oceanic and atmospheric conditions indicate a pattern less like La Niña and more like ENSO-neutral, the La Niña event since boreal summer 2020 is likely to have terminated.

In the western equatorial Pacific, subsurface warm water mass is observed, and in the coming months this is expected to migrate eastward and contribute to further warming of SSTs in the eastern part. Easterly wind anomalies in the eastern part are predicted to diminish. JMA's El Niño prediction model predicts that the NINO.3 SST will continue to rise and get closer to normal, and remain near normal in the coming months. In conclusion, it is likely that ENSO-neutral conditions continue through to next autumn (60%).

2. Western Pacific and Indian Ocean

The area-averaged SST in the tropical western Pacific (NINO.WEST) region was below normal in May. The index is likely to gradually get closer to normal in boreal summer, and remain near normal during autumn.

The area-averaged SST in the tropical Indian Ocean (IOBW) region was below normal in May. The index is likely to be below or near normal through to autumn.

(GOTO Atsushi, Tokyo Climate Center)

* The SST normal for the NINO.3 region (5°S – 5°N, 150°W – 90°W) is defined as a monthly average over the latest sliding 30-year period (1991-2020 for this year).

* The SST normals for the NINO.WEST region (Eq. – 15°N, 130°E – 150°E) and the IOBW region (20°S – 20°N, 40°E – 100°E) are defined as linear extrapolations with respect to the latest sliding 30-year period, in order to remove the effects of significant long-term warming trends observed in these regions.

(a) (b)

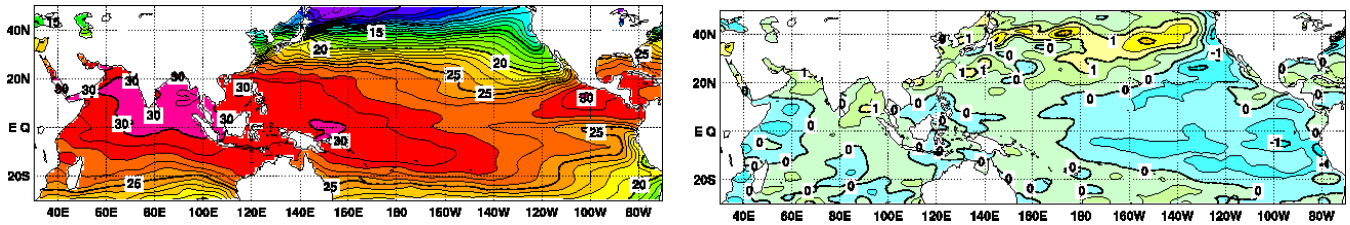

Figure 1-1 Monthly mean (a) sea surface temperatures (SSTs) and (b) SST anomalies in the Indian and Pacific Ocean areas for May 2021

The contour intervals are 1℃ in (a) and 0.5℃ in (b). The base period for the normal is 1991 – 2020.

(a) (b)

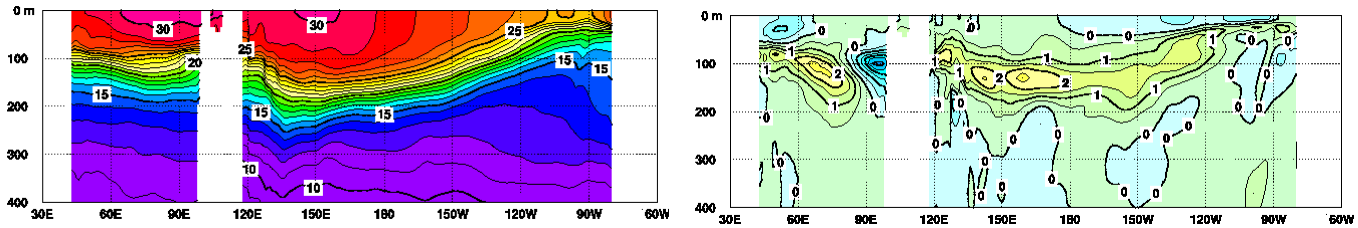

Figure 1-2 Monthly mean depth-longitude cross sections of (a) temperatures and (b) temperature anomalies in the equatorial Indian and Pacific Ocean areas for May 2021

The contour intervals are 1℃ in (a) and 0.5℃ in (b). The base period for the normal is 1991 – 2020.

(a) (b)

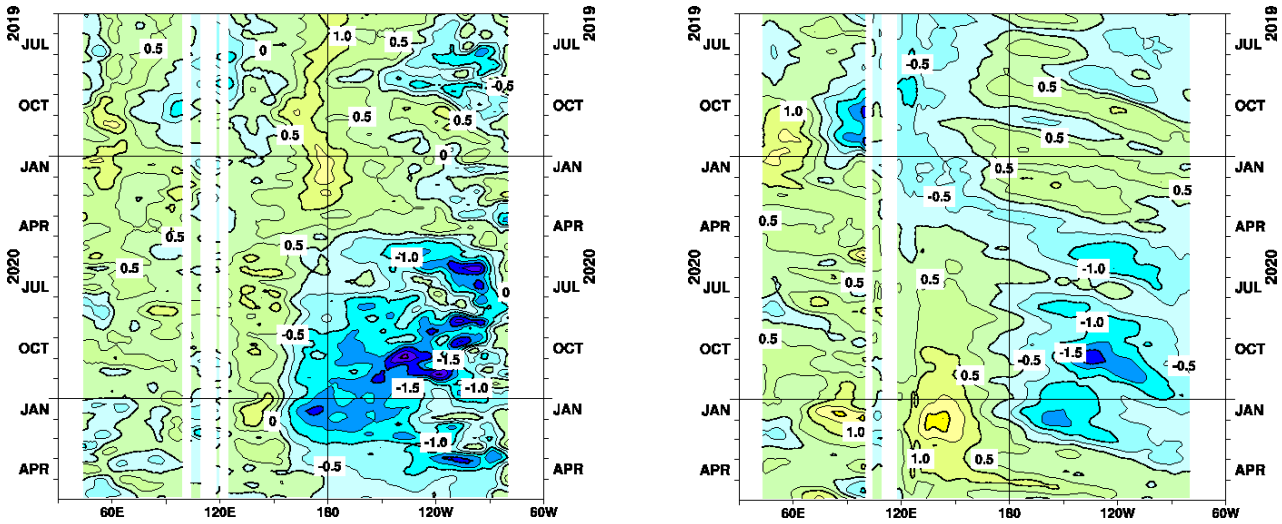

Figure 1-3 Time-longitude cross sections of (a) SST and (b) ocean heat content (OHC) anomalies along the equator in the Indian and Pacific Ocean areas

OHCs are defined here as vertically averaged temperatures in the top 300 m. The base period for the normal is 1991 – 2020.

<<Table of contents <Top of this article

JMA's Seasonal Numerical Ensemble Prediction for Boreal Summer 2021

This report outlines JMA's dynamical seasonal ensemble prediction for boreal summer 2021 (June – August, referred to as JJA), which was used as a basis for JMA's operational warm-season outlook issued on 25 May 2021. The outlook is based on the seasonal ensemble prediction system of the Coupled Atmosphere-ocean General Circulation Model (CGCM). Unless otherwise noted, the base period for the normal is 1981 – 2010.

Summary: Based on JMA's seasonal ensemble prediction system, ENSO-neutral conditions are likely to continue during boreal summer and autumn. In the upper troposphere, large-scale divergence anomalies are predicted from the tropical Indian Ocean to the Maritime Continent, while large-scale convergence anomalies are predicted over the central-to-eastern tropical Pacific. Above-normal precipitation is predicted in and around South Asia and near New Guinea, and below-normal precipitation is predicted near the date line in the tropical South Pacific.

1. SST anomalies (Figure2-1)

Figure 2-1 shows predicted SSTs (contours) and related anomalies (shading) for JJA. Near- or below-normal anomalies are expected in the central-to-eastern equatorial Pacific. Considering that subsurface ocean temperature anomalies in the equatorial Pacific are expected to be small (not shown), ENSO-neutral conditions are likely to continue during the period. The IOBW SST is likely to be below or near normal from boreal spring to autumn.

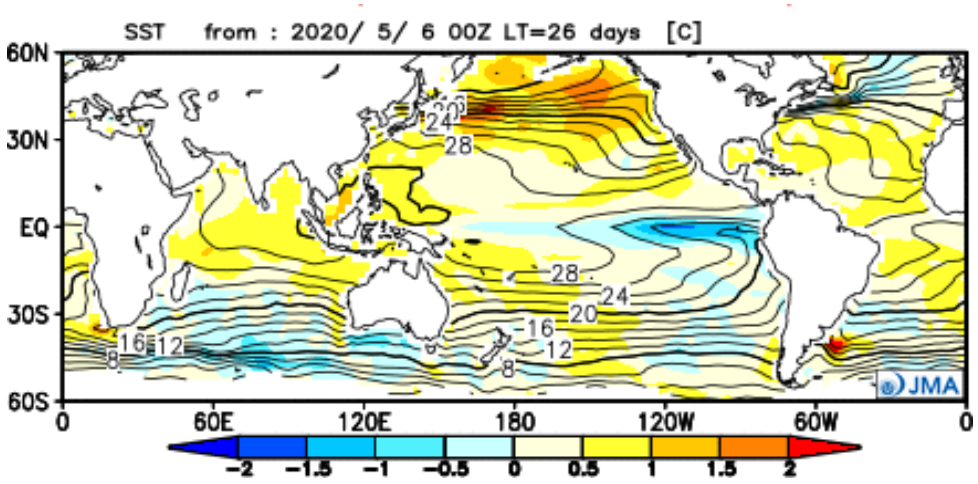

Figure 2-1 Predicted SSTs (contours) and SST anomalies (shading) for June–August 2021 (ensemble mean of 51 members)

2. Prediction for the tropics and sub-tropics (Figure2-2)

Figure 2-2 (a) shows predicted precipitation (contours) and related anomalies (shading) for JJA. Above-normal precipitation is predicted in and around South Asia and near New Guinea, and below-normal precipitation is predicted near the date line in the tropical South Pacific.

Figure 2-2 (b) shows predicted velocity potential (contours) and related anomalies (shading) in the upper

troposphere (200 hPa) for JJA. In association with predicted SST and precipitation anomalies as stated above, negative (large-scale divergence) anomalies are predicted from the tropical Indian Ocean to the Maritime Continent, while positive (large-scale convergence) anomalies are predicted over the central-to-eastern tropical Pacific.

Figure 2-2 (c) shows predicted stream functions (contours) and related anomalies (shading) in the upper troposphere (200 hPa) for JJA. Anti-cyclonic circulation anomalies straddling the equator are predicted from the Atlantic to the Indian Ocean, and cyclonic circulation anomalies straddling the equator are predicted over the central-to-eastern tropical Pacific.

Figure 2-2 (d) shows predicted stream functions (contours) and related anomalies (shading) in the lower troposphere (850 hPa) for JJA. Cyclonic circulation anomalies are predicted from the Middle East to South Asia, and anti-cyclonic circulation anomalies are predicted over southeastern East Asia and the western tropical South Pacific.

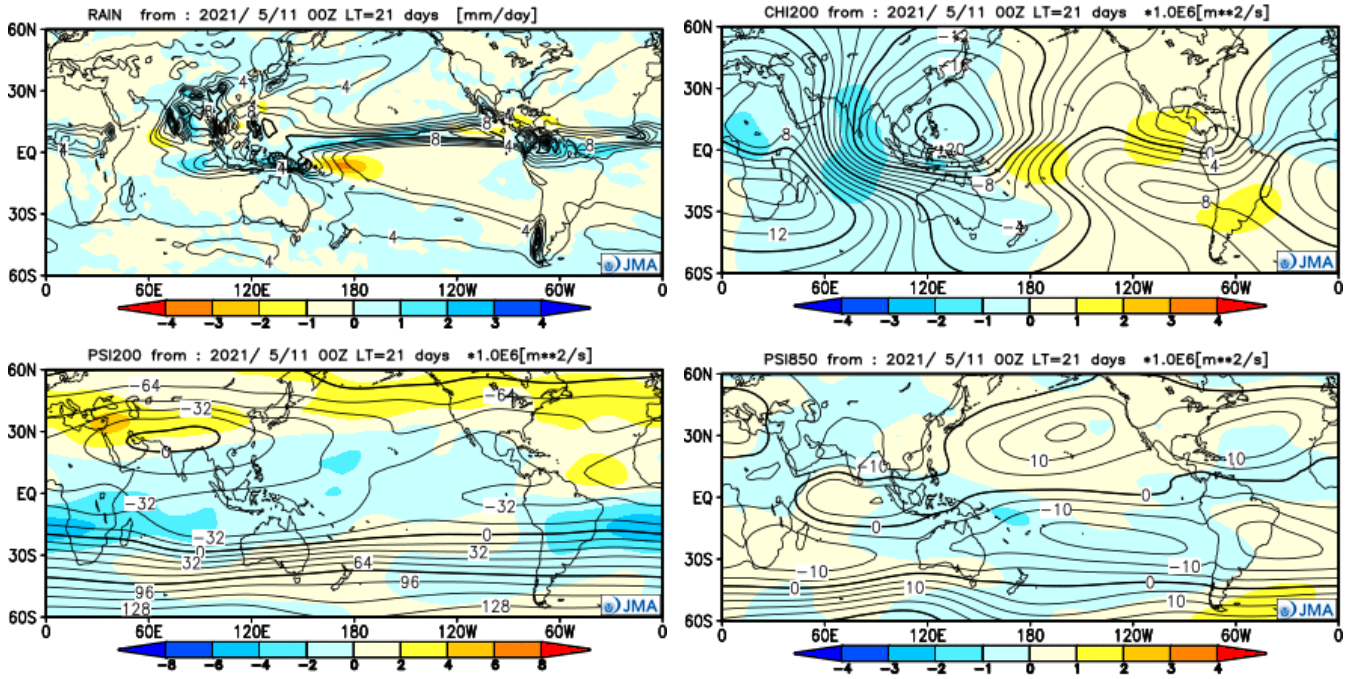

Figure 2-2 Predicted atmospheric fields from 60°N –60°S for June–August 2021 (ensemble mean of 51 members)

(a) Precipitation (contours) and anomaly (shading). The contour interval is 2 mm/day. (b) Velocity potential at 200 hPa (contours) and anomaly (shading). The contour interval is 2×10^6 m^2/s. (c) Stream function at 200 hPa (contours) and anomaly (shading). The contour interval is 16×10^6 m^2/s. (d) Stream function at 850 hPa (contours) and anomaly (shading). The contour interval is 5×10^6 m^2/s.

3. Prediction for the mid- and high- latitudes of the Northern Hemisphere (Figure2-3)

Figure 2-3 (a) shows predicted geopotential heights (contours) and related anomalies (shading) at 500 hPa for JJA. Positive anomalies are predicted over the Northern Hemisphere mid- and high-latitudes, especially over the North Pacific and the North Atlantic.

Figure 2-3 (b) shows predicted sea level pressure (contours) and related anomalies (shading) for JJA. Positive anomalies are predicted from South Asia to the tropical North Pacific, and negative anomalies are predicted over the northern polar region and from Central Asia to northern East Asia.

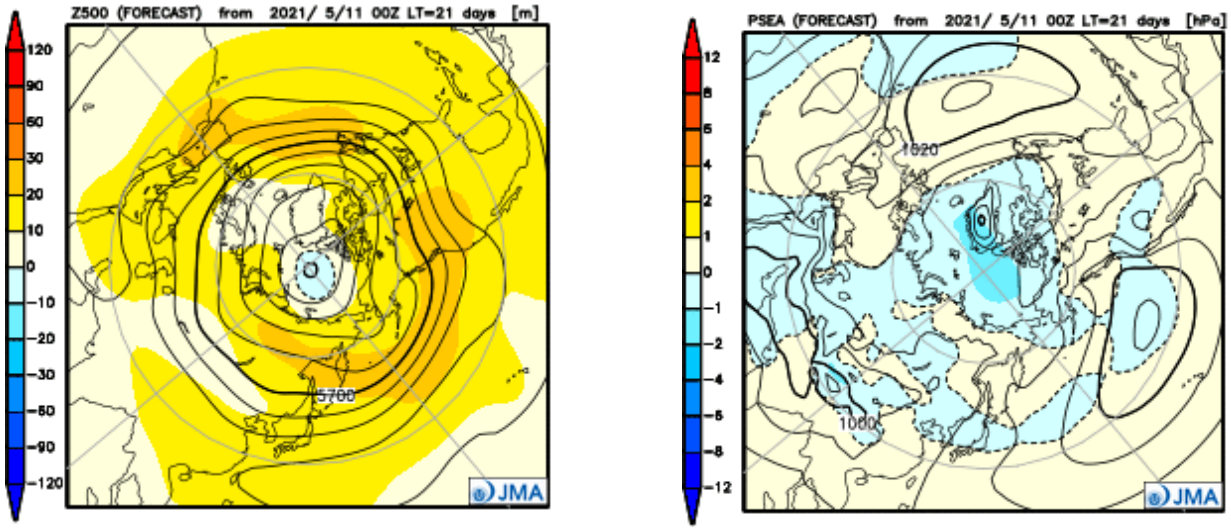

Figure 2-3 Predicted atmospheric fields from 20°N–90°N for June–August 2021 (ensemble mean of 51 members)
(a) Geopotential height at 500 hPa (contours) and anomaly (shading). The contour interval is 60 m. (b) Sea level pressure (contours) and anomaly (shading). The contour interval is 4 hPa.

Note: JMA operates a seasonal Ensemble Prediction System (EPS) using the Coupled atmosphere-ocean General Circulation Model (CGCM) to make seasonal predictions beyond a one-month time range. The EPS produces perturbed initial conditions by means of a combination of the initial perturbation method and the lagged average forecasting (LAF) method. The prediction is made using 51 members from the latest four initial dates (13 members are run every 5 days). Details of the prediction system and verification maps based on 30-year hindcast experiments (1981–2010) are available at http://ds.data.jma.go.jp/tcc/tcc/products/model/.

(GOTO Atsushi, Tokyo Climate Center)

<<Table of contents <Top of this article

Summary of the 2020/2021 Asian Winter Monsoon

This report summarizes the characteristics of the surface climate and atmospheric/oceanographic considerations related to the Asian winter monsoon for 2020/2021.

Note: The Japanese 55-year Reanalysis (JRA-55; Kobayashi et al. 2015) atmospheric circulation data and COBE-SST (Ishii et al. 2005) sea surface temperature (SST) data were used for this investigation. NOAA Interpolated Outgoing Longwave Radiation (OLR) data (Liebmann and Smith 1996) provided by the U.S. NOAA Earth System Research Laboratory (ESRL) from their web site at https://www.esrl.noaa.gov/psd/ was referenced to infer tropical convective activity. The base period for the normal is 1981 to 2010. The term "anomaly" as used in this report refers to deviation from the normal.

1. Surface climate conditions

In winter 2020/2021, three-month mean temperatures were above normal from South Asia to East Asia and below normal from Central Asia to southern Siberia. Clear intra-seasonal temperature anomaly variations were seen from Central to East Asia, where temperatures were low or very low in December and high or very high in February (Figure 3-1). Thus, the East Asian Winter Monsoon (EAWM) was stronger than normal in the first half of winter 2020/2021 and weaker in the second half. Winter precipitation was above normal in and around southern Central Siberia and from the southern part of South Asia to central Southeast Asia, and below normal in and around southern Central Asia. The wetter-than-normal conditions observed in Southeast Asia were consistent with typical anomaly patterns observed in past La Niña events. Drier-than-normal conditions were observed from northern Central Asia to northwestern East Asia and in the eastern part of East Asia in December, while wetter-than-normal conditions were observed in February (Figure 3-2).

Figure 3-3 shows extreme climate conditions for the period between December 2020 and February 2021. Extremely high temperatures were seen from southern India to southwestern China in January and from northwestern South Asia to the eastern part of East Asia in February. Extremely low temperatures were seen in and around southern Central Asia and from Mongolia to northern China in December. Extremely high precipitation was observed in and around central Southeast Asia and southern India in January and from southern Western Siberia to southern Central Siberia in February. Extremely low precipitation was observed in and around the central part of Central Asia in December and in and around southern Central Asia in January.

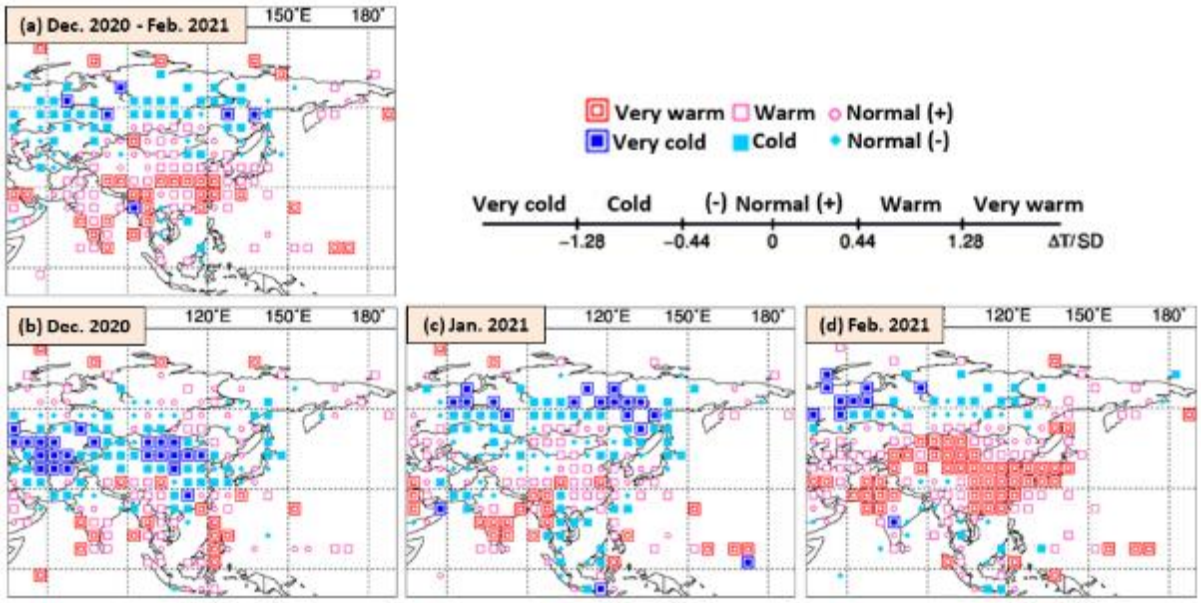

Figure 3-1 Temperature anomalies for (a) December 2020 to February 2021, (b) December 2020, (c) January 2021 and (d) February 2021

Categories are defined by the three-month/monthly mean temperature anomaly against the normal divided by its standard deviation and averaged in 5° × 5° grid boxes. The thresholds of each category are-1.28,-0.44, 0, +0.44 and +1.28. Standard deviations were calculated from 1981- 2010 statistics. Areas over land without graphical marks are those where observation data are insufficient or where normal data are unavailable.

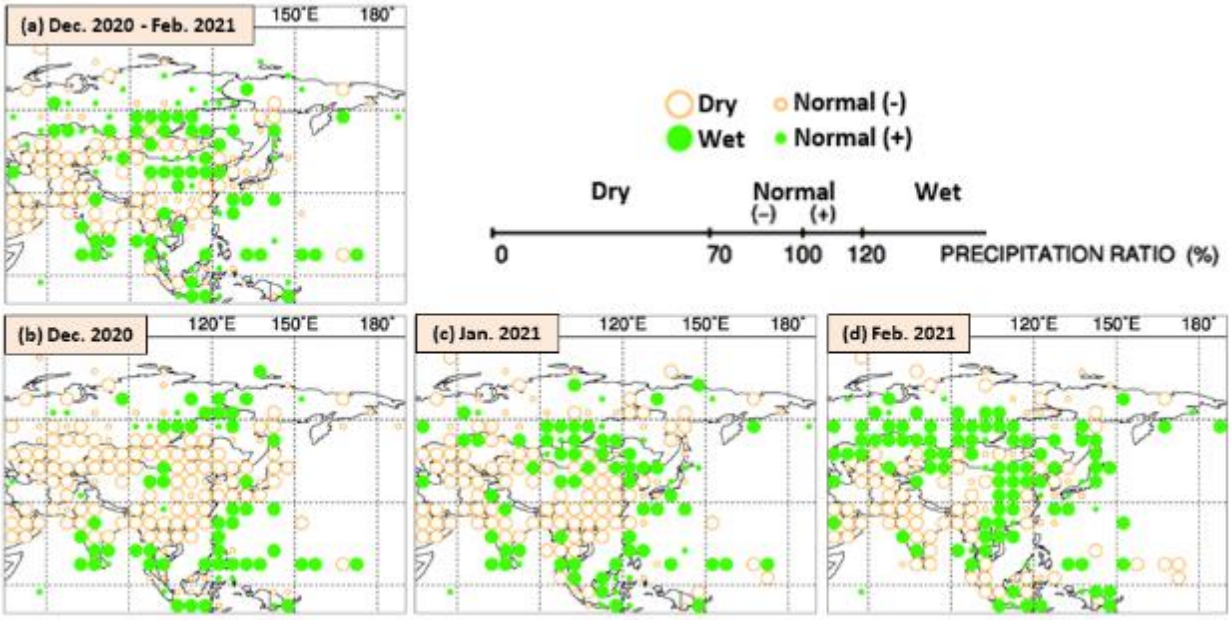

Figure 3-2 Precipitation ratio for (a) December 2020 to February 2021, (b) December 2020, (c) January 2021 and (d) February 2021

Categories are defined by the three-month/monthly precipitation ratio against the normal and averaged in 5° × 5° grid boxes. The thresholds of each category are 70, 100 and 120%. Areas over land without graphical marks are those where observation data are insufficient or where normal data are unavailable.

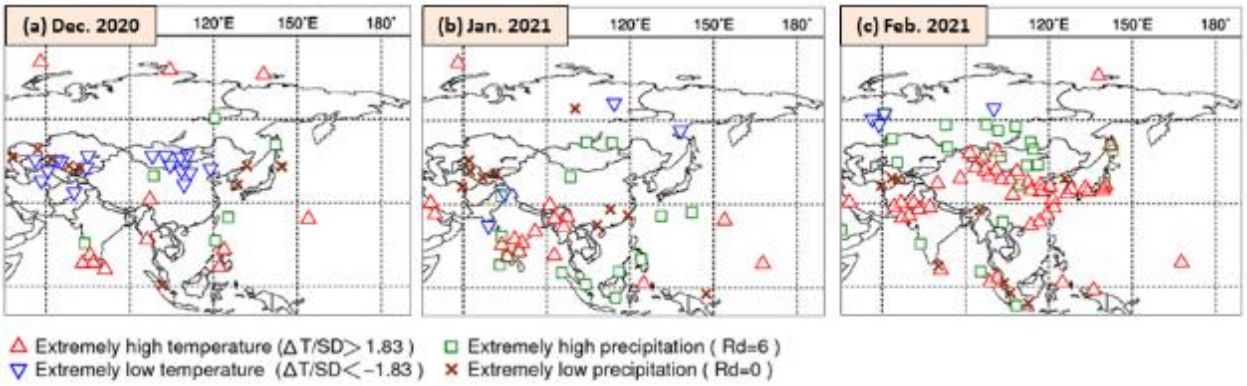

Figure 3-3 Extreme climate stations for (a) December 2020, (b) January 2021 and (c) February 2021

ΔT, SD and Rd indicate temperature anomaly, standard deviation and quintile, respectively.

2. Characteristic atmospheric circulation and oceanographic conditions

This section describes the characteristics of atmospheric circulation and oceanographic conditions in both halves of winter 2020/2021 against a background of distinct intra-seasonal EAWM change.

2.1 Conditions in the tropics

In the equatorial Pacific, remarkably positive SST anomalies were observed west of 150°E, and remarkably negative anomalies were observed from east of 160°E to the central part, in association with the La Niña event that had persisted since boreal summer 2020. In the Indian Ocean, positive SST anomalies observed from the central to eastern part of the northern tropical region and from the area near Madagascar to northwest of Australia decreased during winter (Figure 3-4 (a), (b)). Convective activity inferred from OLR in the first half of the season was enhanced from the central tropical Indian Ocean to the Maritime Continent, reflecting higher-than-normal SSTs in these regions, and was suppressed around the date line in the equatorial Pacific (Figure 3-4 (c)). In the second half of the season, enhanced convection was observed from the eastern part of the Maritime Continent to the Philippines (Figure 3-4 (d)).

Figure 3-5 shows 200- and 850-hPa stream function fields for the first and second halves of winter. In the first half, clear upper-level anti-cyclonic circulation anomalies were seen over southern Eurasia in response to enhanced convective activity from the central tropical Indian Ocean to the Maritime Continent, which enhanced Rossby wave propagation accompanying southward meandering of the subtropical jet stream (STJ) over the eastern part of East Asia (Figure 3-6 (a)). In the second half, the STJ meandered northward over the eastern part of East Asia (Figure 3-6 (b)). This meandering is partly attributed to enhanced convection from the eastern part of the Maritime Continent to the Philippines.

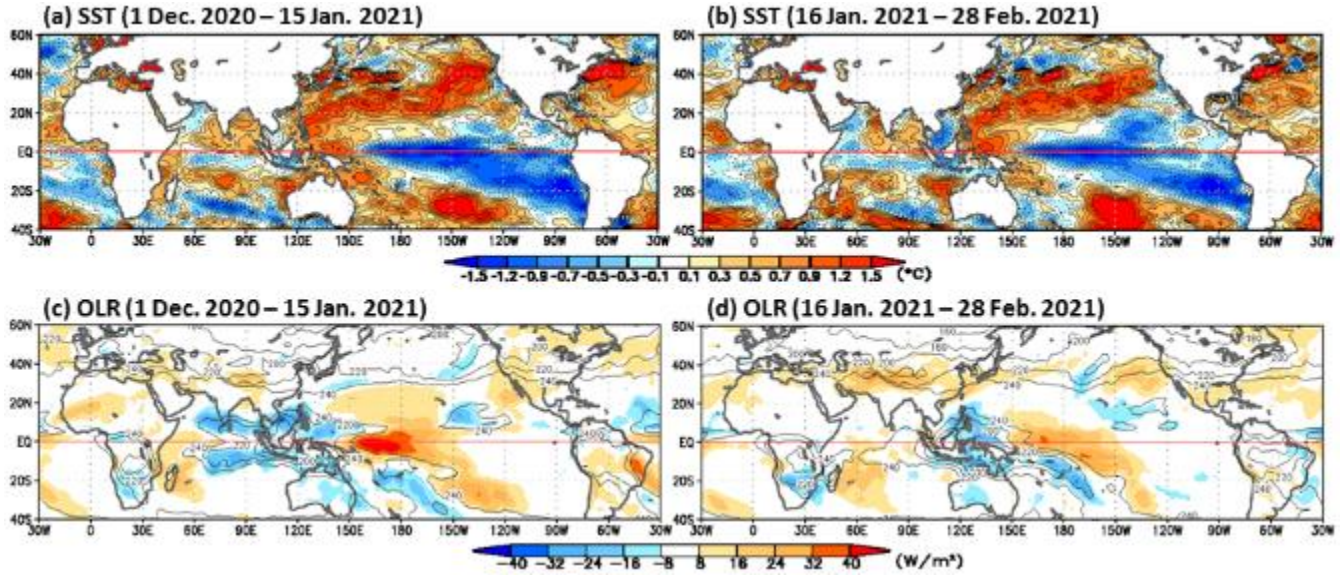

Figure 3-4 SST and OLR for 1 December 2020 to 15 January 2021 and 16 January to 28 February 2021

(a), (b) Shading shows SST anomalies [°C]. (c), (d) Contours indicate OLR at intervals of 20 W/m2, and shading shows OLR anomalies. Negative (cold color) and positive (warm color) OLR anomalies show enhanced and suppressed convective activity compared to the normal, respectively.

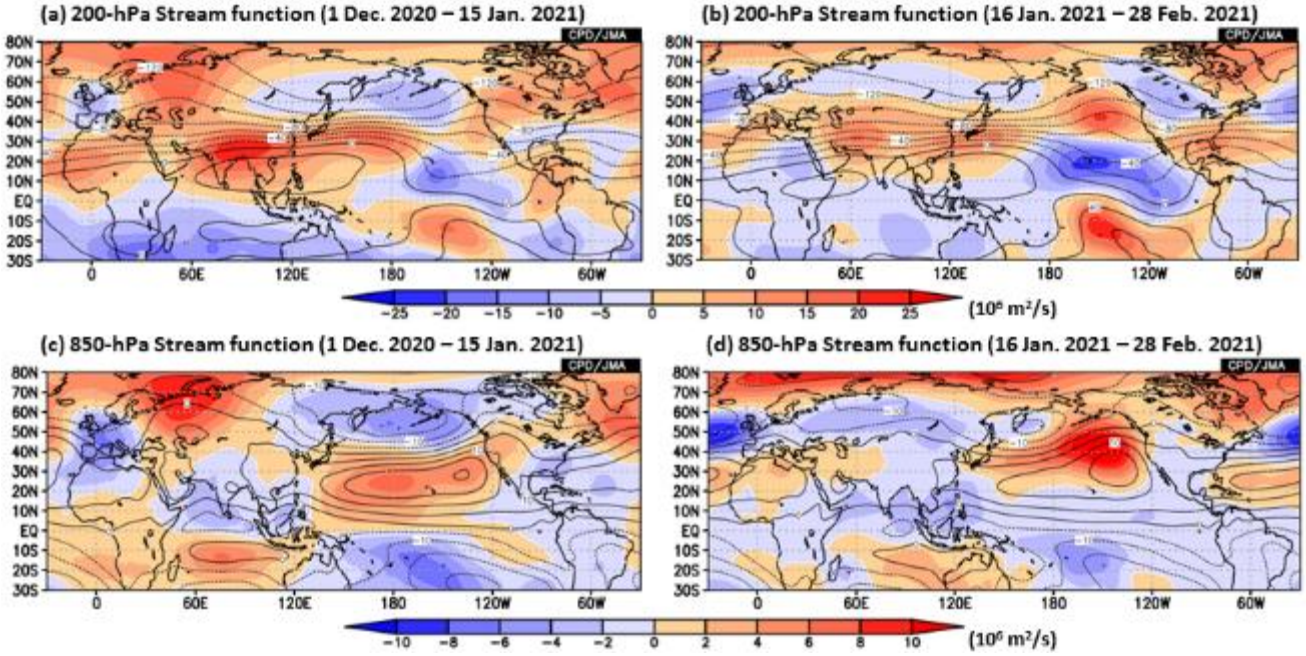

Figure 3-5 As per Figure 3-4, but for 200- and 850-hPa stream function

Contours indicate stream function at intervals of (a) (b) 20 × 106 m2/s and (c) (d) 5 × 106 m2/s, and shading shows stream function anomalies.

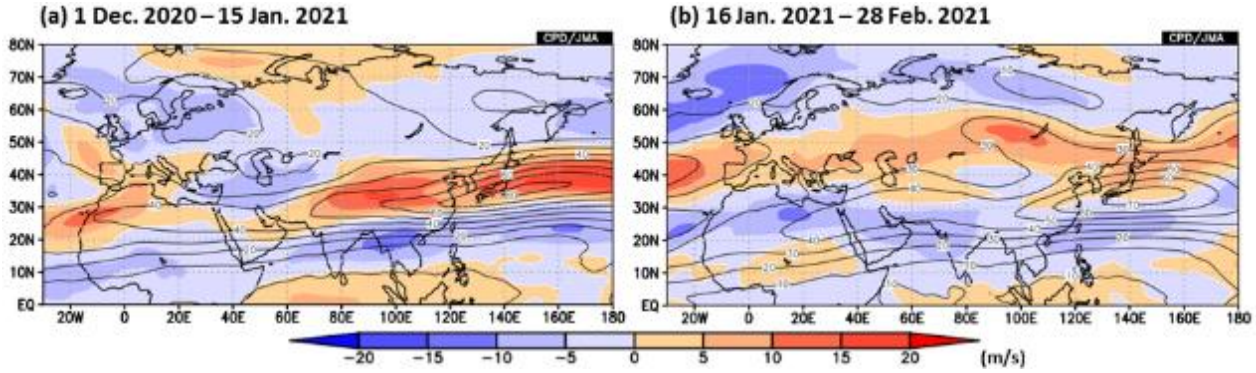

Figure 3-6 As per Figure 3-4, but for 250-hPa wind speed

Contours indicate wind speed at intervals of 10 m/s, and shading shows wind speed anomalies.

2.2 Conditions in the extratropics

The tropospheric polar vortex in the Northern Hemisphere was split into Siberian and North American parts throughout the winter. The polar front jet stream (PFJ) over Eurasia exhibited meandering in the first half of winter, but became clear and showed limited meandering near 50°N in the second half.

Figure 3-7 shows 500-hPa height and sea level pressure in the Northern Hemisphere. In the first half of the season there was a prominent wave train from the North Atlantic to northern Eurasia with a persistent blocking high over Western Siberia, which was possibly attributable to less-than-normal sea ice extents in the Barents Sea (e.g., Mori et al. 2014). Clear negative 500-hPa height anomalies were seen from northeastern East Asia to the northern North Pacific in association with the southward meandering of the PFJ over the region. Corresponding to these upper-level anomaly patterns, the Siberian High and the Aleutian Low were stronger than normal in sea-level pressure fields, indicating a stronger-than-normal EAWM. Lower-level tropospheric temperatures were below normal over eastern Eurasia (Figure 3-8 (a)).

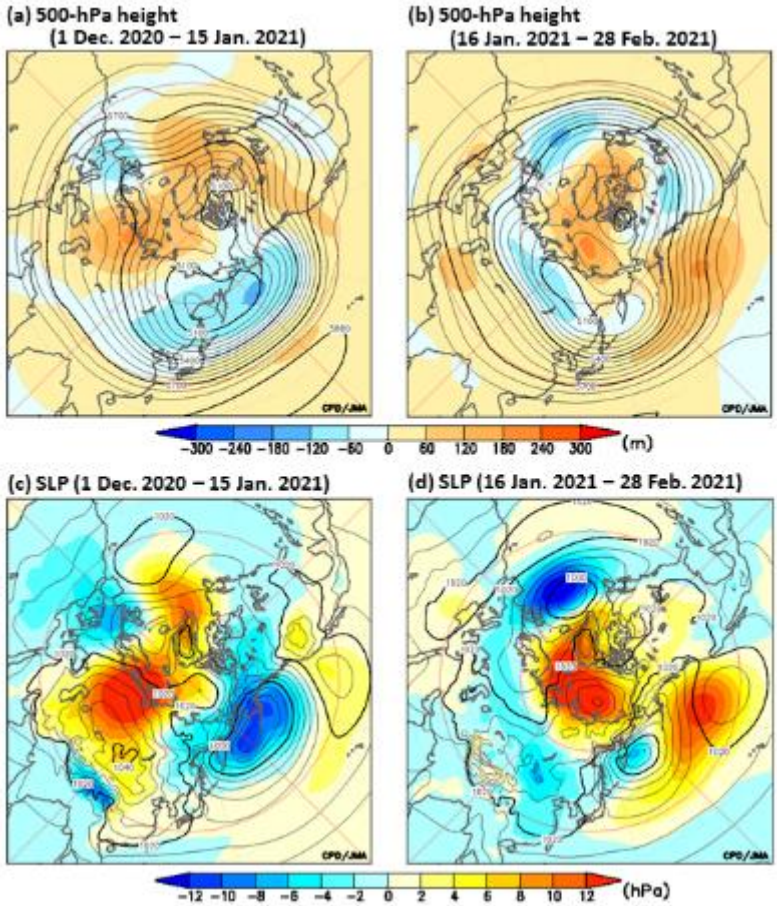

Figure 3-7 As per Figure 3-4, but for 500-hPa height and sea level pressure (SLP)

Contours indicate (a), (b) 500-hPa height at intervals of 60 m, and (c), (d) SLP at intervals of 4 hPa. Shading denotes related anomalies.

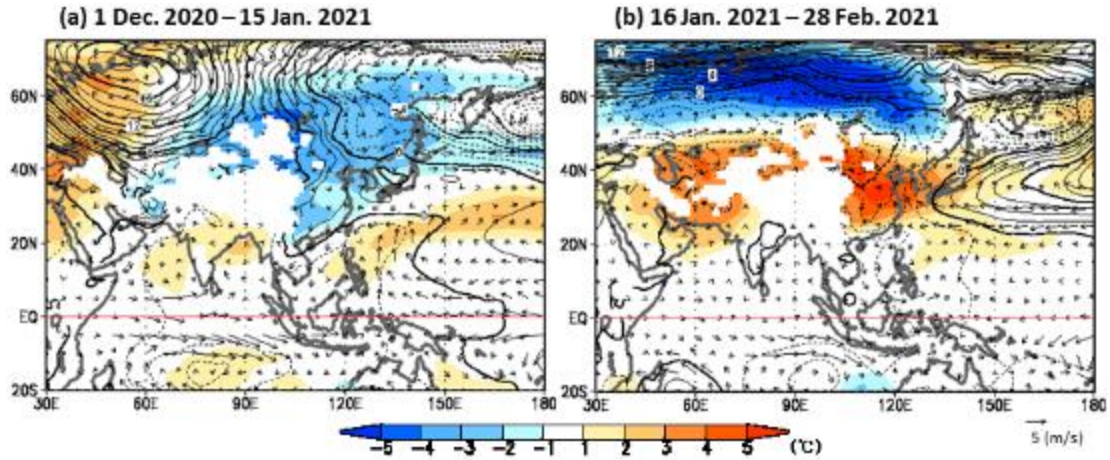

Figure 3-8 As per Figure 3-4, but for SLP anomalies, 850-hPa temperature anomalies and 925-hPa wind anomalies

Contours indicate SLP anomalies at intervals of 1 hPa, and shading shows 850-hPa temperature anomalies [°C]. Vectors denote 925-hPa wind anomalies [m/s].

In the second half of the season, zonally elongated positive anomalies were seen in 500-hPa height fields from southern Europe to East Asia, and negative anomalies were seen over northern Eurasia (Figure 3-7 (b)). Temperatures at 850 hPa were above normal over a wide area from Central to East Asia and below normal north of 50°N over Eurasia (Figure 3-8 (b)). These anomalies were consistent with a clear and non-meandering PFJ near 50°N over Eurasia (Figure 3-6 (b)), which may be linked to a stratospheric sudden warming event occurring from January to early February. In the sea level pressure field, the Siberian High was weaker than normal and the Aleutian Low was shifted northwestward of its normal position (Figure 3-7 (d)), indicating a weaker-than-normal EAWM that contributed to the warm conditions observed in Central and East Asia.

(SATO Hitoshi, Tokyo Climate Center)

References

Ishii, M., A. Shouji, S. Sugimoto and T. Matsumoto, 2005: Objective analyses of sea-surface temperature and marine meteorological variables for the 20th century using ICOADS and the Kobe Collection. *Int. J. Climatol.*, **25**, 865-879.

Kobayashi, S., Y. Ota, Y. Harada, A. Ebita, M. Moriya, H. Onoda, K. Onogi, H. Kamahori, C. Kobayashi, H. Endo, K. Miyaoka, and K. Takahashi, 2015: The JRA-55 Reanalysis: General specifications and basic characteristics. *J. Meteor. Soc. Japan*, **93**, 5 – 48.

Liebmann, B., and C. A. Smith, 1996: Description of a complete (interpolated) outgoing longwave radiation dataset. *Bull. Amer. Meteor. Soc.*, **77**, 1275–1277.

Mori, M., M. Watanabe, H. Shiogama, J. Inoue, and M. Kimoto, 2014: Robust Arctic sea-ice influence on the frequent Eurasian cold winters in past decades. *Nat. Geosci.,* **7**, 869-873.

<<Table of contents <Top of this article

TCC and WMC Tokyo co-contributions to Regional Climate Outlook Forums

WMO Regional Climate Outlook Forums (RCOFs) bring together national, regional and international climate experts on an operational basis to produce regional climate outlooks based on input from participating NMHSs, regional institutions, Regional Climate Centres (RCCs) and global producers of climate predictions. By providing a platform for countries with similar climatological characteristics to discuss related matters, these forums ensure consistency in terms of access to and interpretation of climate information.

In spring 2021, experts from TCC and the World Meteorological Centre (WMC) Tokyo gave presentations on climate outlooks and TCC activities at the following RCOFs, which were held online due to the ongoing COVID-19 pandemic.

- the 17th session of the Forum on Regional Climate Monitoring, Assessment and Prediction for Regional Association II (FOCRA II-17)
- the 19th summer session of the South Asian Climate Outlook Forum (SASCOF-19)
- the 20th North Eurasian Climate Outlook Forum (NEACOF-20)

As part of collaborative activities between TCC and WMC Tokyo, the experts from TCC and WMC Tokyo provided summer season outlooks including probabilistic forecasts based on JMA's dynamical seasonal ensemble prediction system as well as Copernicus Climate Change Service (C3S) multi-model ensemble prediction, which the Japan Meteorological Agency (JMA) has joined in since October 2020. The presenters also covered climate monitoring and forecast products available on the TCC website. These activities are intended to support the output of country-scale outlooks by National Meteorological and Hydrological Services (NMHSs), contribute to the summarization of consensus outlooks and reduce climate disaster risks in the water, agriculture and health sectors for each target area. TCC and WMC Tokyo are committed to collaboration with operational climate communities to enhance progress in forecast skill and application of climate information toward the resolution of common issues and realizing a climate-resilient world.

(WAKAMATSU Shunya, Tokyo Climate Center)

<<Table of contents <Top of this article

You can also find the latest newsletter from Japan International Cooperation Agency (JICA).
JICA's World (April 2021)
https://www.jica.go.jp/english/publications/j-world/2104.html
JICA's World is the quarterly magazine published by JICA. It introduces various cooperation projects and partners along with the featured theme. The latest issue features "South Asia: The Beat of 1.8 Billion People".

Any comments or inquiry on this newsletter and/or the TCC website would be much appreciated.
Please e-mail to tcc@met.kishou.go.jp.
(Editors: KAKIHARA Koichiro and WAKAMATSU Shunya)

Tokyo Climate Center, Japan Meteorological Agency
3-6-9 Toranomon, Minato City, Tokyo 105-8431, Japan

TCC Website:
https://ds.data.jma.go.jp/tcc/tcc/index.html

<<Table of contents